THE JOURNAL OF PHYSICAL CHEMISTRY A

Article

What Controls Selectivity of Hydroxyl Radicals in Aqueous Solution? – Indications for a Cage Effect

Frank-Dieter Kopinke, and Anett Georgi

J. Phys. Chem. A, **Just Accepted Manuscript** • DOI: 10.1021/acs.jpca.7b05782 • Publication Date (Web): 28 Sep 2017

What Controls Selectivity of Hydroxyl Radicals in Aqueous Solution? – Indications for a Cage Effect

Frank-Dieter Kopinke*, Anett Georgi

Department of Environmental Engineering, Helmholtz Centre for Environmental Research – UFZ, Permoserstrasse 15, D-04318 Leipzig, Germany

* *Correspondence to:* F.-D. Kopinke, e-mail: frank-dieter.kopinke@ufz.de

ABSTRACT:

The oxidation of three isotopologues of methylcyclohexane (MCH: C_7H_{14}, C_7D_{14}, c-C_6D_{11}-CH_3) by OH radicals (•OH) in aqueous solution was investigated. *Inter*molecular and *intra*molecular H/D kinetic isotope effects (KIE = $k_H : k_D$) for the abstraction of H- and D-atoms by •OH were measured. These KIEs reflect *inter*- and *intra*molecular selectivities of hydrogen abstraction, i.e. the selection of •OH attack on carbon-hydrogen bonds in different molecules and in different positions of one molecule, respectively. The *inter*molecular selectivity of •OH attack in aqueous solution is largely discriminated against in comparison with the *intra*molecular selectivity. The observed extent of discrimination cannot be explained by partial diffusion control of the overall reaction rates. A cage model, where •OH and hydrocarbon molecules are entrapped in a solvent cage, is more appropriate. The much higher intramolecular KIEs compared to the intermolecular KIEs of the same chemical reaction, R-H + •OH → R• + H_2O, indicate a high degree of mobility of the two reaction partners inside the solvent cage. This mobility is sufficient to develop an intramolecular selectivity comparable to gas-phase reactions of •OH. Furthermore, literature data on KIEs of H-abstraction by •OH in aqueous and gas phase, respectively, are discussed. There is a general tendency towards lower selectivities in the aqueous phase.

INTRODUCTION

Hydroxyl radicals (•OH) play an important role as highly reactive oxidants in environmental and engineered compartments.[1,2] This is true for gas-phase processes[3-5] as well as for reactions in aqueous environments.[6,7] Therefore, it is useful to know and to understand their selectivity patterns in various reactions. Hydrogen abstraction is the dominant reaction pathway for attack of •OH on saturated hydrocarbons. From the literature, it is known that the selectivity pattern of •OH may be significantly different for the same class of reactions in the gas phase than in the water phase.[4,8-17] This could be attributed to (i) different inherent reactivities of •OH in the two media (e.g. due to solvation effects in the water phase) or to (ii) a diffusion limitation of reaction events due to very high rate coefficients.[17] Rudakov et al.[18] interpret the selectivity pattern of •OH in aqueous solution by means of a cage effect according to eq. 1:

$$\mathrm{RH} + \bullet\mathrm{OH} \underset{k_{-1}}{\overset{k_1}{\leftrightarrows}} \{\mathrm{RH}\cdots\mathrm{OH}\}^* \overset{k_2}{\rightarrow} \mathrm{R}\bullet + \mathrm{H_2O} \qquad (1)$$

where {RH···OH}* is the oriented encounter complex in the water cage. This cage model is similar to the model of Minakata et al.[17] where an initial van der Waals complex between the reactants with a significant energy sink is postulated. Rudakov et al.[18] based their cage model on kinetic isotope effects (KIEs) measured in aqueous- and gas-phase oxidation of cyclohexane isotopologues: KIE = k_{C6H12}/k_{C6D12} = 1.18 in water and 2.57 in the gas phase, both at 298 K, where k_{C6H12} and k_{C6D12} are observed (apparent) second-order rate coefficients of cyclohexane oxidation. Therefore, these ratios are named apparent KIEs (AKIEs).[19] The oxidation systems considered were selected such that the cyclohexane conversion was dominated by the attack of •OH. Based on the different KIEs, the H-abstraction by •OH is much more selective in the gas phase than in the water phase.

It is worth to clearly define selectivity parameters: The *inter*molecular selectivity of a bimolecular reaction - such as H-abstraction - is usually described by the ratio of apparent second order rate constants $k_A : k_B$ in a mixed substrate system (A + B + •OH). It reflects how selective a reactive species - such as •OH - discriminates *between different substrate molecules* (A vs. B). The closer this ratio is to a value of one, the lower the intermolecular selectivity. The *intra*molecular selectivity reflects the discrimination of the same reactive species between different positions *within one molecule*, e.g. between different types of C-H-

bonds, such as those on primary (RCH_2-H), secondary (R_2CH-H) or tertiary (R_3C-H) carbon atoms. Intramolecular selectivities can also be described by relative rate constants, e.g. $k_{\text{primC-H}} : k_{\text{secC-H}} : k_{\text{tertC-H}}$ which are transferred into relative reactivities $r_{\text{primC-H}} : r_{\text{secC-H}} : r_{\text{tertC-H}}$ by normalization to one C-H-bond ($r_i = k_i/n_i$ with n_i as number of equivalent C-H-bonds in a certain position). The correlation between intra- and intermolecular selectivities can be examined by comparing the two selectivity parameters on hand of an appropriate pair of hydrocarbons, e.g. cyclohexane (= $[CH_2]_6$) and neopentane (= $[CH_3]_4C$): $k_{\text{cyclohexane}} : k_{\text{neopentane}} \approx r_{\text{secC-H}} : r_{\text{primC-H}}$. This approximation is based on the assumptions that the reactivity of a molecule can be described as the sum of reactivities of all C-H-bonds in that molecule. One reason for failing of this correlation between inter- and intramolecular selectivities can be a (partial) diffusion control of reaction rates.

The cage-effect concept was originally introduced by Frank and Rabinowich.[20] It is able to explain plausibly a low intermolecular selectivity of •OH, because the solvent cage increases the reaction probability between the two entrapped species irrespective of the inherent substrate reactivity. The reactants keep closely together for a longer time window. However, this entrapment does not predict intramolecular selectivities, i.e. the selection of reaction sites inside a substrate molecule. In the framework of the cage model, the intramolecular selectivity depends on the mobility of the two reacting species (substrate molecules and •OH) inside the solvent cage. The time window for their reorientation is determined by the life-time of hydrogen bonded water molecule clusters, which is about 100 ps.[21] This time window is about a thousand times longer than the time between molecular vibrations of entrapped solute molecules ($\tau_{\text{vibration}} = h/k_B T \approx 0.1$ ps, with h and k_B as Planck's and Boltzmann's constants, respectively). The contact time of the reactants may become much longer if one assumes either binding interactions in the van der Waals complex between the reactants[17] or a significant promotion of water clustering by dissolved nonpolar solutes.[21]

The aims of the present study are (i) to measure intra- and intermolecular selectivities of H-abstraction by •OH, (ii) to understand the correlation between these two selectivities on a mechanistic level, and (iii) to elucidate the extent of intramolecular selectivity of H-abstraction that can be developed by •OH attack on saturated hydrocarbons in aqueous solution. Knowing and understanding reaction selectivities is one way to gain insight into the nature of oxidizing species in a complex reaction system.

A plausible way to determine intramolecular selectivities is the quenching of hydrocarbon radicals R• followed by analysis of the quenching products according to eq. 2:[22]

$$\text{R-CH}_2\text{-R'} + \bullet\text{OH} \xrightarrow{-\text{H}_2\text{O}} \text{R-}\overset{\bullet}{\text{C}}\text{H-R'} \xrightarrow{\text{O}_2} \xrightarrow{\varepsilon_i} \text{Products, such as R-CH(OH)-R'} \quad (2)$$

wherein $\varepsilon_i = 0 \ldots 1$ is a transfer factor which describes the yield of a product *i* formed from the precursor alkyl radical R•. Unfortunately, in most cases it is not easy to find an appropriate sequence of quenching and stabilization reactions which allows quantitative relations between product yields and primary radical positions to be calculated.[2,23]

CONCEPT OF THE ISOTOPE METHOD

In the present study, we followed a different approach to measure intra- and intermolecular selectivities of hydrogen abstraction. It is based on the measurement of KIEs in the Fenton oxidation of deuterated isotopologues of methylcyclohexane (MCH) as substrates, namely C_7H_{14} (MCH-D_0), c-C_6D_{11}-CH_3 (MCH-D_{11}) and C_7D_{14} (MCH-D_{14}). We measured relative reaction rates ($k_{\text{MCH-D0}} : k_{\text{MCH-D11}} : k_{\text{MCH-D14}}$) and relative product yields obtained by quenching and stabilization of the alkyl radicals produced by primary •OH attack. The concept is illustrated in chapter 1 of the SI part. Absolute product yields do not allow a 1:1 assignment to relative reactivities of the various C-H-bonds in MCH, because we do not know the various transfer factors ε_i, nor can we assume that they all are equal. However, for our approach it is only necessary that the observed products represent unambiguously the place of the primary •OH attack on the MCH molecule. For example, 4-methylcyclohexanone (4-MCH-one) and 4-methylcyclohexanol (4-MCH-ol) are definitely products from an •OH attack at the 4-position of the MCH-ring. This assignment neglects intra- and intermolecular radical isomerization reactions, which is justified due to the fast bimolecular quenching of alkyl radicals by dissolved oxygen. The quantitative information in our approach results from the isotope effects on the product yields. The relative product yields from the various isotopologues reflect the different reactivities of the corresponding C-H- and C-D-bonds, i.e. the intramolecular KIEs of the H- or D-abstraction by •OH. In this concept it is assumed that the reactivity of a secondary C-D-bond in the cyclohexane ring is equal in MCH-D_{14} and MCH-D_{11}, which is certainly a reasonable assumption. Furthermore, observed KIEs in poly-deuterated compounds may be composed of primary and secondary KIEs (KIE caused by the presence of C-D-bonds in the vicinity of the reaction site). Minor contributions of secondary KIEs may slightly affect the absolute values of measured KIEs (e.g. in comparison to mono-deuterated isotopologues), but do not challenge the concept.

The rationale of the applied technique can be summarized as follows: in order to measure intramolecular selectivities of radical attack, it is not necessary to know the values of transfer

factors ε_i from various alkyl radicals to the corresponding detectable products. Instead, it is sufficient to detect a set of products which have equal transfer factors for different isotopologues of the same substrate molecule. This is a less demanding requirement than those for selectivity analyses from product yields.

MATERIALS AND METHODS

The deuterated MCHs were from CDN Isotopes (distributed by EQ Laboratories GmbH, Augsburg, Germany). All other chemicals were obtained at the highest purity from Sigma-Aldrich or Merck (Germany).

All oxidation experiments were performed as batch experiments in 250 mL glass bottles, filled with 235 mL of 0.5 mM aqueous H_2SO_4 (pH = 3.0) and closed with Mininert-valves™ at ambient temperature (22 ± 2°C). The bottles were extensively purged with pure oxygen and spiked with 2 to 4 µL of MCHs (in total about 130 µM, which is below the maximum water solubility of 155 µM). After manual shaking for several minutes, the headspace over the water phase was analyzed (50 µL gas-tight microsyringe) by means of GC-MS. Headspace analyses are based on the direct proportionality between water and gas phase concentrations of the analytes. 18 µmol Fe^{2+} (as $FeSO_4$ solution) and 18 µmol H_2O_2 (= 77 µM each in the reaction solution) were then added separately (t = 0). The bottle was manually vigorously shaken after each spiking. After a few minutes, headspace samples were taken and analyzed. For the following 30 minutes the reaction bottles were continuously shaken on a horizontal shaker. After the final headspace analysis, the bottle was spiked again with the same amounts of $FeSO_4$ and H_2O_2 and handled in the same way; the whole procedure was repeated several times. This procedure (series A), wherein binary or ternary mixtures of isotopologues were oxidized, produced data for the determination of relative rate constants of isotopologues.

After a number of reaction periods, residual peroxides were quenched by adding an excess (about 10 mmoles) of thiosulfate. Then, the bottle was opened and 10 mL of dichloromethane (containing 10 ppm of chlorobenzene as internal GC standard) was added for a final liquid-liquid extraction. After several minutes of manual shaking, the two-phase mixture was saturated with NaCl (for salting-out of organics) and shaken again for 5 min. After separation of the first extract, the extraction procedure was repeated with another 10 mL of dichloromethane. The two extracts were dried over Na_2SO_4 and analyzed separately by means of GC-MS (QP2010 from Shimadzu, SCAN mode, 60 m x 0.32 mm capillary column DB624, 1.8 µm film thickness, T_{GC} = 30°C (3 min), then 4 to 10 K/min up to 250°C). GC-MS analyses of gas samples were usually performed under isothermal conditions (T_{GC} = 30°C) in

the SIM mode for characteristic fragments in order to determine the various MCH isotopologues more precisely and more sensitively.

In another batch experiment (series B), after each oxidation step an aliquot of the aqueous reaction mixture (5 mL) was withdrawn, quenched for residual H_2O_2 and peroxides (500 µL methanol, 10 mg thiosulphate), and extracted with 5 mL of dichloromethane for GC-MS analysis. The reaction bottle was refilled with 5 mL of clean water in order to keep the volumes constant. These analyses provided information about the variability of product yields during MCH conversion (cf. Fig. S3).

For detailed GC-MS product analyses, three separate oxidation experiments were conducted (series C), each with 150 µM of one of the dissolved MCH-isotopologues. After a two-step oxidation (2 x 60 µM stoichiometric Fenton-reagent, 2 x 30 min reaction time), the MCH conversion degree was about 25 ± 5%. Each reaction bottle was amended with 10 mL of dichloromethane (containing 100 ppm chlorobenzene as internal standard) and shaken manually for 1 min. About 30 g of NaCl was then added and the bottle was shaken for 5 min. After withdrawal of the solvent, an additional 10 mL of dichloromethane was added, shaken again for 5 min, and removed. The two solvent extracts were dried over Na_2SO_4 and analyzed by means of GC-MS. The identification of the oxidation products was possible on the basis of their characteristic mass spectra taken from literature libraries. For the assignment of *cis-trans*-isomers of the MCH-ols, their tabulated boiling points were taken into account (cf. Fig. S2).

The ratio of the analyte concentrations in the two extracts provides information about the completeness of the extraction. For the hydrophobic component MCH, the ratio $C_{1st\ extract}$: $C_{2nd\ extract}$ was ≥50. For the most hydrophilic components, MCH-ols, it was about 10, indicating that ≥90% of them were caught in the combined dichloromethane extracts.

The GC-MS analysis of the combined extracts allows: (i) the identification of the oxidation products formed, (ii) the determination of their isotopic composition, and (iii) a semi-quantitative mass balance of the oxidation. This balance is based on the approximation that all components including MCH are extracted with equal efficiencies and have equal (molar) response factors in the GC-MS analyses (TIC peak areas in the SCAN mode). Although not exactly fulfilled, these approximations are considered to be reasonable. The mass balance indicates that about 80% of the converted MCHs are detected as MCH-ones, -al, and -ols. About 20% of the converted MCHs are oxidation products in the form of a cluster of $C_7H_{10\text{-}12}O_2$ compounds, but these could neither be fully resolved nor structurally identified.

RESULTS AND DISCUSSION

The oxidation experiments were designed in such a way that the MCH conversion was mainly controlled by •OH attack (stoichiometric amounts of Fe^{2+} and H_2O_2). Figure S1 shows a typical conversion profile of MCH-D_0 in a multi-step oxidation experiment. It is evident that the major conversion takes place immediately after addition of the stoichiometric Fenton reagent. Further slow reactions are negligible. This type of kinetics is in agreement with the expected fast production of •OH by the Fenton reaction, according to $Fe^{2+} + H_2O_2 \rightarrow Fe^{3+} +$ •OH + OH^-, whereas consecutive reactions (catalytic Fenton cycle) play only a minor role. Initially, 1 µmol of H_2O_2 gives rise to the conversion of about (0.3 ± 0.1) µmol of MCH under the applied conditions. We carried out some control measurements with photochemical activation of H_2O_2 (254 nm) which yielded identical intermolecular KIEs (data not published here). Therefore, we have reason to rely on the stoichiometric Fenton reagent as a suitable source to study KIEs of •OH reactions.

Intermolecular KIEs, cage effect and diffusion control

The results from oxidation experiments with three MCH isotopologues applied as a mixture in aqueous solution (series A) are presented in Figure 1. Equ. 3 is a linearization of an apparent first-order competition kinetics:

$$\frac{d \ln C_\mathrm{A}}{d \ln C_\mathrm{B}} = \frac{k_\mathrm{A}}{k_\mathrm{B}} \times \frac{1 - X_\mathrm{A,gas}}{1 - X_\mathrm{B,gas}} \approx \frac{k_\mathrm{A}}{k_\mathrm{B}} \qquad (3)$$

where C_A, C_B are normalized concentrations of two MCH isotopologues measured at a certain reaction time and k_A, k_B the corresponding second-order rate coefficients. Equ. 3 contains a correction term for the gas-phase fractions of MCH ($X_\mathrm{i,gas}$) which are not available for OH attack in the aqueous phase. One can show, however, that its effect is negligible under the applied conditions (cf. SI part, chapter 6). According to equ. 3 for two competing reactions of •OH, the slopes of the two regression lines in double-logarithmic coordinates are the ratios of rate coefficients $k_\mathrm{MCH\text{-}D0} : k_\mathrm{MCH\text{-}D14} = 1.072 \pm 0.003$ and $k_\mathrm{MCH\text{-}D11} : k_\mathrm{MCH\text{-}D14} = 1.007 \pm 0.003$. The given scattering intervals correspond to two standard deviations. The regression lines are strictly linear through 4 orders of magnitude in the MCH concentrations, i.e. up to >99.99% MCH conversion.

Obviously, the intermolecular selectivity of •OH attack on MCH isotopologues in water is very low. The value $k_\mathrm{C7H14} : k_\mathrm{C7D14} = 1.072$ is in perfect agreement with data from Pignatello

et al.[25], who measured k_{C6H12} : k_{C6D12} = 1.06-1.08 (at 298 K) for oxidation of cyclohexanes in water with two different OH-dominated oxidation systems (Fe^{2+}/H_2O_2 and UV/H_2O_2). For comparison, the KIEs for •OH attack on secondary C-H-bonds in the gas phase are k_{C6H12} : k_{C6D12} = 2.5 and k_{C5H10} : k_{C5D10} = 2.8.[26]

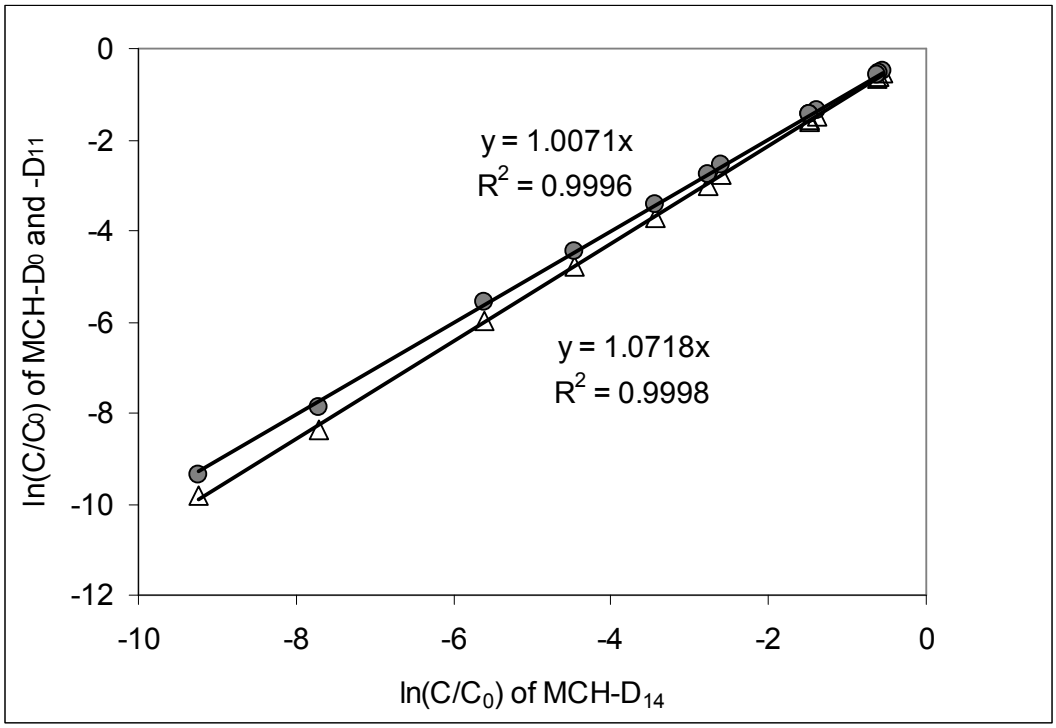

Figure 1. Rayleigh plot of the Fenton oxidation of methylcyclohexane isotopologues in aqueous solution ($C_{0,i}$ = 43 μM each, series A experiments): (Δ) for MCH-D_0 vs. MCH-D_{14} and (●) for MCH-D_{11} vs. MCH-D_{14}. Error bars for singe data points are smaller than the size of the point symbols.

It is reasonable to question whether the hypothesis of a cage effect is necessary in order to explain small AKIEs. An alternative explanation could theoretically be a partial diffusion control of the overall reaction rates. Let us check the validity of this explanation from a quantitative point of view. From the simple model of a reversible diffusion step followed by an irreversible reaction step (equ. 1) we can derive equ. 4:[17]

$$k_{\text{obs}} = \frac{k_{\text{chem}} \times k_{\text{diff}}}{k_{\text{chem}} + k_{\text{diff}}} = \frac{k_{\text{chem}}}{\mathbf{1} + \boldsymbol{k_{\text{chem}}/k_{\text{diff}}}} \qquad (4)$$

with k_{obs}, k_{chem}, and k_{diff} as second-order rate coefficients of the total reaction (observed rate), the chemical reaction step (true reaction rate without diffusion limitation), and the diffusion-

limited (maximal) rate constant, respectively. One can interconvert the terminology of rate coefficients in eqs. 1 and 4 by the following relations: $k_{obs} = k_2 \times k_1 / (k_2 + k_{-1})$, $k_{chem} = k_2 \times k_1/k_{-1}$ and $k_{diff} = k_1$. We call the term in bold in eq. 4, i.e. $1/(1 + k_{chem}/k_{diff})$, the 'attenuation factor', because it decreases the observed rate coefficient. Minakata et al. estimated $k_{diff} \approx (1.15 \pm 0.02) \times 10^{10}$ L/(mol s), which is close to the highest observed rate coefficients for •OH reactions in the aqueous phase.[11] Equ. 4 can be resolved towards k_{chem}, yielding equ. 5:

$$k_{\text{chem}} = \frac{k_{\text{obs}} \times k_{\text{diff}}}{k_{\text{diff}} - k_{\text{obs}}} = \frac{k_{\text{obs}}}{\mathbf{1 - k_{obs}/k_{diff}}} \qquad (5)$$

We call the term in bold in equ. 5, i.e. $1/(1 - k_{obs}/k_{diff})$, the 'amplification factor', because it increases the true chemical rate constant. Now one can check to what extent the diffusion limitation attenuates the true $KIE_{chem} = k_{chem,H}/k_{chem,D}$ towards an observable diffusion-affected $AKIE_{predicted} = k_{obs,H}/k_{obs,D}$ on the basis of the example C_6D_{12} vs. C_6H_{12} with the following rate constants (values from [11,16,18], all in terms of 10^9 L/(mol s)): $k_{diff} = 11.5$, $k_{obs,C6H12} = 6.0$, $k_{obs,C6D12} = 5.2$, $AKIE_{experimental} = 1.15$, see also SI part).

$$\text{AKIE}_{\text{predicted}} = \frac{\text{KIE}_{\text{true}}}{\frac{(1 - k_{\text{obs}}/k_{\text{diff}})_{\text{C6D12}}}{(1 - k_{\text{obs}}/k_{\text{diff}})_{\text{C6H12}}}} = \frac{\text{KIE}_{\text{true}}}{\frac{(1 - 5.2/11.5)}{(1 - 6.0/11.5)}} = \frac{\text{KIE}_{\text{true}}}{1.15} \qquad (6)$$

The calculation shows that partial diffusion control of hydrogen abstraction from cyclohexane by •OH can only explain about a 15% attenuation of the true KIE. Assuming KIE_{true} to be equal or at least close to the KIE observed in the gas phase, $KIE_{gas\ phase} = 2.5$,[26] according to equ. 6 we obtain $AKIE_{predicted} = 2.5/1.15 \approx 2.2$. This value is significantly higher than $AKIE_{experimental}$ of 1.15 determined by Rudakov et al.[18] or 1.07 determined by Pignatello et al.[25] Actually, the discrimination is much higher when considering the ratio of enrichment factors.[19] Enrichment factors compare the extent of isotope fractionation as deviation from a non-fractionating process, i.e. KIE = 1.0. In this terminology predicted and experimental isotope fractionation differ by a factor of $(KIE_{true} - 1) / (AKIE - 1) = (2.5 - 1) / (1.15 \text{ to } 1.07 - 1) = 10 \text{ to } 20$. Hence, partial diffusion control cannot be the only, and certainly not the main, reason for the low observed intermolecular AKIEs. A similar assessment can be made for the MCH isotopologues C_7H_{14} and C_7D_{14} investigated in the present study (see SI part).

Therefore, another explanation is necessary. The cage model, which postulates a longer contact time between the reactants than predicted by the free-diffusion model, is able to

explain the measured kinetics. This can be illustrated by means of the above given relationship $k_{obs} = k_2 \times k_1 / (k_2 + k_{-1})$. The cage effect, which is equivalent to a low back-diffusion rate coefficient k_{-1}, yields $k_{obs} \approx k_1$, i.e. the observable rate coefficient is approximately equal to the diffusion rate coefficient k_1 but does not reflect the chemical rate coefficient k_2. Diffusion is usually a less fractionating process than a chemical reaction. Therefore, the true chemical isotope fractionation is discriminated.

Recently, Richnow et al.[27] studied carbon and hydrogen KIEs resulting from the attack of OH-radicals on 13 benzene derivatives in aqueous solution. They explain unexpectedly low AKIEs owing to masking effects, caused by pre-equilibria between the substrate and •OH (π-complexes), preceding the rate limiting step. This explanation is similar to the van der Waals complexes proposed in [17] and the cage effect favored in the present study. π-complex formation is limited to unsaturated substrates and, therefore, cannot be applied to •OH attack on alkanes, as investigated in the present study. A careful inspection of the data set in [27] reveals that the magnitude of observed AKIEs correlates with the polarity of the substrate molecules rather than with their reactivity: Nonpolar substrates such as benzene and alkylbenzenes have small AKIEs ($AKIE_C$ = 1.002 – 1.006), whereas benzene derivatives substituted by a polar functional group such as nitrobenzene, anilines, and benzonitrile have relatively large AKIEs ($AKIE_C$ = 1.02 – 1.03). This finding is fully in line with the cage model: Non-polar substrates are subject of a pronounced cage effect, whereas solvation of polar groups diminishes cage formation. The interpretation of hydrogen AKIEs is more complex, because addition of OH-radicals to the aromatic ring and hydrogen abstraction from side chains expose opposite KIEs (inverse vs. normal, respectively). Nevertheless, the observed $AKIE_H$ follow a similar ranking between nonpolar and more polar substrates, e.g. $AKIE_H$ = 1.03 for o-xylene vs. $AKIE_H$ = 1.40 for dimethylaniline.

Reaction pathways and product pattern

A typical gas chromatogram of extracted oxidation products of MCH (series C experiments) is shown in Figure S2. The sum of yields of O-containing MCH products having the intact cyclohexane ring (c-$C_7H_{14}O$ + c-$C_7H_{12}O$ = alcohols, ketones, aldehydes) was ≥80% of the converted MCH. Less than 10% of fragmented and acyclic oxidation products were detected. These relations give us confidence in the interpretation of the product pattern collected in Table 1. The following simplified reaction sequence can be postulated:

$$Fe^{2+} + H_2O_2 \rightarrow \bullet OH + Fe^{3+} + OH^- \qquad (8)$$

$$\bullet OH + c\text{-}C_7H_{14} \rightarrow c\text{-}C_7H_{13}\bullet + H_2O \quad (9)$$

$$c\text{-}C_7H_{13}\bullet + O_2 \rightarrow c\text{-}C_7H_{13}\text{-}O\text{-}O\bullet \quad (10)$$

$$c\text{-}C_7H_{13}\text{-}O\text{-}O\bullet \rightarrow\rightarrow c\text{-}C_7H_{13}\text{-}OH + c\text{-}C_7H_{12}{=}O + ... \quad (11)$$

In order to interpret the product pattern quantitatively with respect to the site of H/D-abstraction in the MCH molecules, it is necessary to have an overview of the reaction pathways which the MCH radicals ($c\text{-}C_7H_{13}\bullet$) may undergo. A simplified reaction scheme (Figure 2) is adopted from the review of Fokin and Schreiner.[12]

The alkylperoxyl radicals decompose via the following two major reaction pathways: (i) via dimerization and unimolecular decomposition of tetroxides, and (ii) via a 'metal-dependent pathway', whereby dissolved iron assists in the formation and decomposition of hydroperoxides. The most significant source of alcohols may be the Russell reaction, which proceeds as a bimolecular electrocyclic reaction between primary or secondary peroxyl radicals, whereas the formation pathways of the ketones may be more diverse.[23] It is important to state that the position of the functional groups (hydroxyl or carbonyl) in the product molecule is always the same as the site of radical attack in the

Figure 2. Reaction scheme for oxidation of cyclohexane and quenching of primary alkyl radicals with O_2 up to cyclohexanol and -one (modified from Fokin and Schreiner[12]).

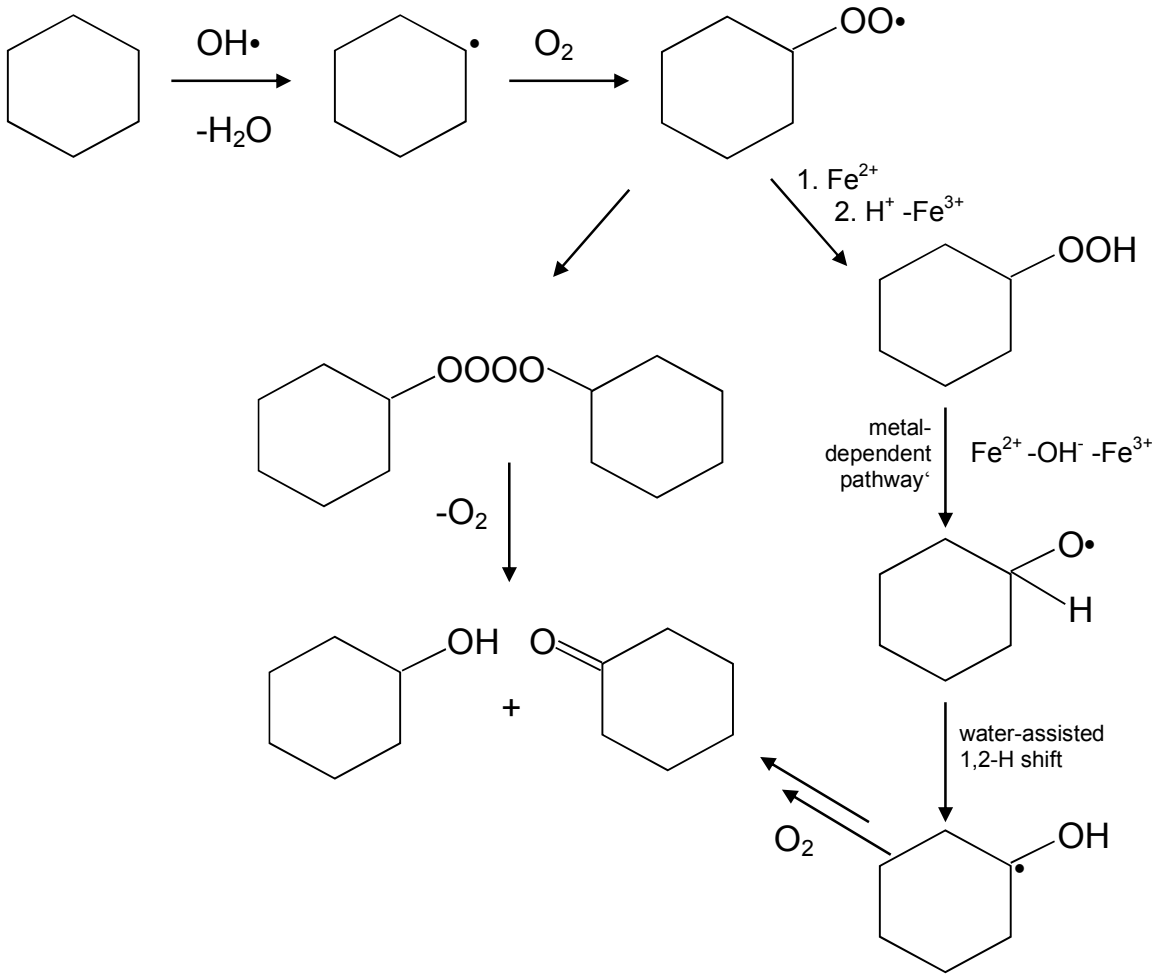

substrate molecule. The various reaction pathways of alkylperoxide radicals in aqueous solution are considered in more detail in several reviews.[2,23] The fate of tertiary alkylperoxide radicals is less well understood. They are candidates for a carbon-chain fragmentation leading to acyclic products from the *tert*-MCH-radical.

Table 1 summarizes relative yields of products from Fenton oxidation of various MCH isotopologues; all are normalized to the yields of 4-MCH-one at about 25% MCH conversion.

Table 1. Relative molar yields of products from Fenton oxidation of various methylcyclohexane isotopologues, normalized to the yields of 4-MCH-ones (average values from two oxidation experiments and three GC-MS analyses each, ± one standard deviation of the mean value) at 25% MCH conversion

Oxidation products	MCH-D_0	MCH-D_{11}	MCH-D_{14}

MCH-ols			
1-MCH-ol 	0.425 ± 0.005	0.343 ± 0.003	0.41 ± 0.05
cis-2-MCH-ol 	0.235 ± 0.015	0.30 ± 0.01	0.38 ± 0.04
trans-2 + cis/trans-3 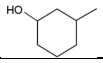	1.06 ± 0.03	1.22 ± 0.01	1.35 ± 0.01
cis/trans-4-MCH-ol 	0.23 ± 0.02	0.33 ± 0.02	0.31 ± 0.01
Cyclohexylmethanol M-MCH-ol 	0.091 ± 0.015	0.244 ± 0.045	0.098 ± 0.022
MCH-ones			
2-MCH-one 	0.90 ± 0.01	0.805 ± 0.005	1.03 ± 0.07
3-MCH-one 	1.99 ± 0.01	2.15 ± 0.05	2.25 ± 0.05
4-MCH-one 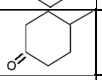	1	1	1
MCH-al 	0.315 ± 0.005	0.57 ± 0.02	0.168 ± 0.010
Product ratios			
∑ MCH-ones / ∑ MCH-ols	2.06	1.86	1.75
Fraction of methyl oxidation products	= (0.091+0.315) / 6.246 = 0.0650	= (0.244+0.57) / 6.962 = 0.117	= (0.098+0.168) / 6.996 = 0.038

In order to interpret the pattern of oxidation products with respect to the site-specificity of the primary radical attack on the MCH molecule, it is necessary to check how sensitive this pattern is with regard to the degree of MCH conversion. Figure S3 shows product selectivities S_i, defined as moles of a product *i* normalized to the sum of moles of formed products *j* ($S_i = n_i/\Sigma n_j$) over a range of MCH conversions from 20 to 80% (series B experiments). The low observed dependency allows us to use the measured product selectivities at about 25% MCH conversion as 'true' primary selectivities without any extrapolation to zero MCH conversion.

Relative reactivities of carbon-hydrogen bonds and intramolecular KIEs

The product analyses in Table 1 are a main outcome of the present study. Therefore, some features will be considered in detail. The carbonyl compounds are the dominant class, amounting to about 2/3 of the MCH oxidation products. The distribution of the three cyclic ketones is similar (in the range of ±10%) for the various MCH isotopologues. This is as to be expected when the site of the initial •OH attack determines the yield pattern. Based on the

number of reactive hydrogen atoms, one would expect a 2 : 2 : 1 distribution for the yields of 2-, 3-, and 4-MCH-one. However, the 2-MCH-one is significantly discriminated against by a factor of about 2. Possible reasons for this discrimination are considered in the SI part. Briefly, the transfer factor ε from 2-methylcyclohexyl radical to 2-MCH-one is lower than for the other secondary methylcyclohexyl radicals.

In contrast to the MCH-ones, the yields of MCH-al resulting from •OH attack at the CH_3- or CD_3-groups are significantly different for the various isotopologues. MCH-D_{11} oxidation yields a factor of 3.4 ± 0.3 more MCH-al than the oxidation of MCH-D_{14}. This factor reflects the intramolecular preference for a primary C-H bond in MCH-D_{11} compared to the corresponding C-D-bond in MCH-D_{14}.

A pattern similar to that for MCH-al is measured for the M-MCH-ol yields: MCH-D_{11} yields a factor of 2.5 ± 1.0 more M-MCH-ol than MCH-D_{14}. This similarity in relative product yields is important with respect to the possible role of a second KIE, which might be involved in the transfer from alkyl radicals to aldehydes and ketones (R-CH_3 → R-CH_2• →→ R-CH=O) due to the scission of a second carbon-hydrogen bond, whereas it should not be relevant in the transfer to alcohols (R-CH_3 → R-CH_2• →→ R-CH_2-OH). Obviously, such a second KIE is not yield-determining. Table 1 contains yields of the various MCH products normalized to the yield of 4-MCH-one for the respective isotopologue. In MCH-D_{11} and -D_{14} (i.e. $C_6D_{11}CH_3$ and $C_6D_{11}CD_3$) the methylene group at 4-position can be considered as identical. Thus, when we consider the combined product yields from •OH attack on the two methyl groups (MCH-al + M-MCH-ol) of MCH-D_{11} and -D_{14}, we obtain a $KIE_{intra,methyl} = k_{CH3}/k_{CD3}$ = (0.57 + 0.244)/(0.168 + 0.098) = 3.1 ± 0.5 (for derivation, see SI part). It is much higher than the apparent intermolecular selectivity $AKIE_{MCH} = k_{C7H14}/k_{C7D14}$ = 1.072 as deduced from the relative oxidation rates of MCH-D_0 and -D_{14}. In mechanistic terms, this means that the •OH inside the water cage or van der Waals complex has sufficient time and mobility to develop at least a significant part of its inherent chemical selectivity for attack on different carbon-hydrogen bonds of an alkane substrate such as MCH.

To the best of our knowledge, there are no KIEs yet available in the literature for site-specific D-abstraction from pure hydrocarbons by •OH radicals in aqueous solution, derived from intramolecular (i.e. non-discriminating) competition experiments. Relevant literature data for small and polar molecules such as alcohols and ethers are compiled in Table S1. Although most of these data are based on intermolecular competition, kinetic data for small and rather polar molecules such as ethanol and glycine probably reflect a less affected •OH selectivity, because these molecules are less prone to cage-effects than hydrocarbons in aqueous solution.

Bonifacic et al.[28] derived the following KIEs: $k_{\mathbf{CH3}\text{-CH2OH}}$: $k_{\mathbf{CD3}\text{-CD2OH}}$ = 3.4 and $k_{\text{CH3-}\mathbf{CH2}\text{-OH}}$: $k_{\text{CD3-}\mathbf{CD2}\text{-OH}}$ = 1.96 (data published without error ranges). The methylene group in the glycine anion reacts with a KIE = $k_{\text{NH2-}\mathbf{CH2}\text{-COO-}}$: $k_{\text{NH2-}\mathbf{CD2}\text{-COO-}}$ = 1.6 (with •OH in H_2O) to 2.0 (with •OD in D_2O).[29] The KIE value for the methyl group in ethanol is close to our (intramolecular) value for the methyl group in MCH (3.4 vs. 3.1). These KIEs are still lower than measured for OH• attack on methyl groups in the gas phase ($KIE_{methyl,gas}$ = 4.6 at 300 K).[12] This decreased selectivity of •OH attack is in line with a general trend towards lower selectivity in aqueous-phase H-abstractions compared with gas-phase reactions. If one compares the H-abstraction selectivity of •OH in terms of relative rate constants $k_{primC\text{-}H}$: $k_{secC\text{-}H}$: $k_{tertC\text{-}H}$, one can take the following representative ratios: in the gas phase 1 : 13 : 65[10] and in the aqueous phase 1 : 5 : 23.[17] Apparently, OH-radicals abstract H-atoms in aqueous solution with a lower selectivity than in the gas phase. This is the same conclusion as deduced from a comparison of KIEs.

Summarizing all these data, we conclude that the measured intramolecular KIE for hydrogen abstraction from the methyl group in MCH, i.e. k_{CH3}/k_{CD3} = 3.1, supports the view that OH-radicals can develop their full intramolecular selectivity inside the postulated water cage.

Taking into account all the site-specific products from Table 1 which can be unambiguously assigned to the abstraction of a hydrogen or deuterium atom from the MCH molecules, relative reactivities per C-H- or C-D-bond ($k_{C\text{-}H}$ or $k_{C\text{-}D}$) were calculated, normalized to the reactivity of the corresponding carbon-hydrogen bond in the 4-position of the cyclohexane ring, and are collected in Table 2 and Figure S4; they reflect the potential and limitations of calculations based on product analyses.

Table 2. Relative reactivities of carbon-hydrogen bonds $k_{C\text{-}H}$ and $k_{C\text{-}D}$ calculated from site-specific product patterns

	MCH-D_0		MCH-D_{11}		MCH-D_{14}	
Positions of H abstraction in the MCH molecule	Site-specific product ratios[1)]	$\boldsymbol{k_{C\text{-}H}}$	Site-specific product ratios	$\boldsymbol{k_{C\text{-}H/D}}$	Site-specific product ratios	$\boldsymbol{k_{C\text{-}D}}$
1, 1 tertiary C-H	0.425	**0.69**	0.343	**0.52**	0.41	**0.63**
2, 4 secondary C-H	0.835 + 0.90	**0.71**	0.86 + 0.805	**0.63**	1.11 + 1.03	**0.82**
3, 4 secondary C-H	0.46 + 1.99	**1.00**	0.66 + 2.15	**1.06**	0.62 + 2.25	**1.10**
4, 2 secondary C-H	0.23 + 1.00	**1.00**	0.33 + 1.00	**1.00**	0.31 + 1.00	**1.00**
Methyl, 3 primary C-H	0.091 + 0.315	**0.22**	0.244 + 0.57	**0.41**	0.098 + 0.29	**0.135**

1) Relative molar product yields from Table 1, added values are yields of MCH-ols + MCH-ones/-als

It may be useful to compare these data with those from incremental methods, whereby a set of relative reactivities ('group rate constants' × 'group contribution factors') is derived from a broad set of kinetic data. The two most recent incremental models, those of Minakata et al.[15-17] and of Monod et al.,[13,14] yield $k_{\text{primC-H}} : k_{\text{secC-H}} : k_{\text{tertC-H}}$ = 1 : 5.1 : 23 and 1 : 3.4 : 5.9, respectively. Although using the same (or similar) data basis, the two models did not generate identical rate increments. Nevertheless, they both yield a selectivity pattern of •OH that reflects a lower selectivity in the aqueous- compared to the gas-phase reaction (cf. data above). The product-yield-based values from Table 2 for the Fenton oxidation of MCH in water yield a different reactivity pattern, with $k_{\text{primC-H}} : k_{\text{secC-H}} : k_{\text{tertC-H}}$ = 1 : 4.5 : 3.1. Obviously, our product analysis discriminates strongly against the reactivity of the tertiary C-H-bond in MCH. This may be due to the formation of ring-splitting products from the tertiary peroxide radical, although these were not positively identified. Therefore, we consider this value as biased. However, the relative reactivity of a secondary C-H-bond in 3- and 4-position of the MCH ring ($k_{\text{secC-H}}$ = 4.5) in the water cage reaction is within the range of increment values from literature.

When considering the product distribution from MCH-D_0 and -D_{14}, one might expect similar patterns, because all carbon-hydrogen bonds are uniform throughout the molecules: either C-H- or C-D-bonds. However, a significant difference in the yields of the two aldehydes is obvious from Table 2. This can be explained on the basis of different KIEs for primary and secondary carbon-hydrogen bonds, which lead to a higher contribution of the methyl group to the overall reactivity of MCH in the nondeuterated than in the perdeuterated isotopologue.

KIE of •OH attack on secondary carbon-hydrogen bonds

The comparison of product yields from MCH-D_{11} ($C_6D_{11}CH_3$) and -D_{14} ($C_6D_{11}CD_3$) enabled us to calculate the intramolecular KIE for hydrogen abstraction from the methyl group (cf. above). The 'normalization sites' in these two molecules are the (identical) secondary C-D-bonds in the cyclohexane ring. In a similar way, the comparison between product yields from MCH-D_{11} and -D_0 can be used to determine the intramolecular KIE for hydrogen abstraction from ring-methylene groups. In this case, the 'normalization site' is the CH_3-group common to both molecules. Using the normalized product yields from Table 1, we obtain $\text{KIE}_{\text{intra,methylene}} = \Sigma S_{\text{i-MCH-D0}} / \Sigma S_{\text{i,MCH-D11}} \times \Sigma S_{\text{l,MCH-D11}} / \Sigma S_{\text{l,MCH-D0}}$ = (0.235 + 1.06 + 0.23 + 0.90 + 1.99 + 1) / (0.30 + 1.22 + 0.33 + 0.805 + 2.15 + 1) x (0.244 + 0.57) / (0.091 + 0.315) = 1.87 ± 0.3, where the indices *i* and *l* represent all products from ring methylene groups and from the CH_3-group, respectively. When we consider only the 4-position in the MCH ring, we

obtain $KIE_{intra,4\text{-}methylene}$ = (1 / 1) x (0.244 + 0.57) / (0.091 + 0.315) = 2.00 ± 0.2, which is not significantly different from the averaged KIE-value. These intramolecular KIE values for the abstraction of a secondary hydrogen from MCH in water are slightly lower than that for the gas-phase oxidation ($KIE_{secC\text{-}D,gas}$ = 2.6).[12] This is the same tendency as observed for KIE for primary carbon-hydrogen bonds: OH-radicals attack less selectively in aqueous solution than in the gas phase.

Comparison of inter- and intramolecular KIEs in gas- and water-phase reactions

In order to provide a comprehensive survey, about 30 KIE values for hydrogen abstraction by •OH radicals, determined in the present study or taken from literature sources, are collected in Table S1. If the cage model adequately reflects the reality, then the extent of discrimination of KIEs should decrease for less reactive and more hydrophilic, small molecules, i.e. AKIE values should be higher. Considering the few available KIE data from the literature,[30] this prediction is more-or-less confirmed: $k_{CH3OH} : k_{CD3OH}$ = 2.25,[11] $k_{C2H5OH} : k_{C2D5OH}$ = 1.93[28] and 1.58,[11] $k_{\mathbf{CH3}\text{-}NH2} : k_{\mathbf{CD3}\text{-}NH2}$ = 1.86,[26] $k_{NH2\text{-}\mathbf{CH2}\text{-}COO\text{-}} : k_{NH2\text{-}\mathbf{CD2}\text{-}COO\text{-}}$ = 1.6 to 2.0,[28] $k_{acetone\text{-}D0} : k_{acetone\text{-}D6}$ = 4.2,[10] $k_{MTBE\text{-}D0} : k_{MTBE\text{-}D12}$ = 2.0.[31] The KIE measured by Bonifacic et al.[28] for ethanol in water is close to that in the gas phase ($k_{C2H5OH} : k_{C2D5OH}$ = 2.6[32]), but still following the rule that OH-radicals react less selectively in aqueous solution than in the gas phase.

All these data were derived from competition experiments with labelled compounds. In principle, one can also deduce such intermolecular AKIEs from shifts in the natural isotopic composition of the unconverted substrate fraction, i.e. from bulk enrichment factors in OH-driven oxidation reactions.[19] This method has been recently applied to the oxidation of some n-alkyl *tert*-alkyl ethers in aqueous solution, yielding the following AKIEs (which are approximately equivalent to $k_{ether\text{-}D0} : k_{ether,perdeuterated}$): for MTBE = 1.56[33] and 1.69 ± 0.25,[34] for ETBE = 1.34[33] and 1.54 ± 0.10,[34] and for TAME = 1.81 ± 0.39.[34] All these KIEs are significantly higher than those measured with the highly reactive and hydrophobic hydrocarbons, such as cyclohexane and MCH, in accordance with the cage model.

Fokin and Schreiner[12] considered the chemistry of alkane transformations via radical attack in detail, also including the •OH attack and related KIEs. From the data collected in that article for gas-phase reactions, it becomes obvious that the KIEs for deuterium abstraction by •OH are higher for attacked stronger C-D-bonds: KIE_{CD4} = 7.4, $KIE_{primC\text{-}D}$ = 4.6, $KIE_{secC\text{-}D}$ = 2.6, $KIE_{c\text{-}C6D12}$ = 2.6, $KIE_{c\text{-}C5D10}$ = 2.74, $KIE_{tertC\text{-}D}$ = 1.9 (all at 300 K).[12] This trend is explained by the position of the transition state on the reaction coordinate: the more exothermic the reaction is, the earlier the transition state is located, and thus the smaller is the influence of the

strength of the broken carbon-hydrogen bond. Droege and Tully[35] measured $AKIE_{cyclohexane}$ = 2.59 ± 0.16 (at 292 K), Hess and Tully[36] $AKIE_{methanol}$ = 2.15 ± 0.16 (at 293 K), both in the gas phase. The relatively small KIE for methanol fits with the activated state of the methyl C-H-bond due to the geminal OH-group.

Wallington et al.[32] discussed the correlation between gas-phase and aqueous-phase reactivities of •OH for a wide variety of organic compounds, in particular for saturated compounds which are attacked by the same type of reaction: hydrogen abstraction. They found that for oxygenated compounds (ketones, alcohols, ethers, carboxylic acids, esters) and nitriles, the set of logarithmic rate constants in both reaction media are linearly correlated with $\log(k_{aqu}) = -1.80 + 0.85 \times \log(k_{gas})$ (R = 0.95; k in terms of cm^3/(molecules x s)). This correlation demonstrates that the gas-phase and the solution-phase rate constants are essentially identical over almost 4 orders of magnitude in reactivity (for solvated substrates). Non-solvated substrates, such as alkanes and cycloalkanes, all appear to have an enhanced reactivity toward •OH in aqueous solution. The empirical correlation is $\log(k_{aqu}) = 1.93 + 0.54 \times \log(k_{gas})$. The advantage of non-solvated substrates in aqueous solution decreases with increasing molecule size (e.g. k_{aqu}/k_{gas} = 23 for methane vs. 1.1 for n-octane). Wallington et al.[32] interpreted these correlations in terms of collision and transition-state theories as well as association equilibria between hydrocarbons in the condensed and gas phases.[37] They also fit with the cage model, which distinguishes between hydrophilic (solvated) and hydrophobic (non-solvated) molecules.

CONCLUSIONS

In the present study, intermolecular KIEs were measured for Fenton oxidation of MCH isotopologues in aqueous solution. They reveal a very low *inter*molecular selectivity of •OH radical attack on hydrocarbons. Intramolecular KIEs for hydrogen abstraction from the methyl group and from a methylene group in the cyclohexane ring were derived, based on a detailed analysis of oxidation products from various isotopologues. They reveal a high degree of *intra*molecular selectivity of hydrogen abstraction by •OH.

This apparent discrepancy cannot be quantitatively explained by a partial diffusion control of the bimolecular reaction. Instead, a cage model, whereby OH-radicals and hydrocarbon molecules are encapsulated in a solvent cage, is more appropriate. The much higher intramolecular KIEs compared to the intermolecular AKIEs of the same chemical reaction, R-H + •OH → R• + H_2O, indicate a high degree of mobility of the two reaction partners inside the solvent cage. This mobility is sufficient to develop an intramolecular selectivity comparable to that in gas-phase reactions of •OH.

The described phenomenon may have significant implications for interpretation of selectivity patterns of •OH radicals in aqueous solution. It challenges the basic assumption of the group contribution methods for prediction of molecule reaction rate constants, which is the additivity of reactivities of single bonds, groups and structures within a substrate molecule,[4,13-15] for aqueous phase reactions. A pronounced difference between inter- and intramolecular selectivities has been demonstrated for abstraction of H atoms from one hydrocarbon (methylcyclohexane) by OH-radicals in aqueous solution. It remains to be determined whether or not this applies to other substrates and reactive radicals such as Cl• and $SO_4•^-$. For compounds prone to a cage effect, reactivity prediction by the common group contribution methods and vice versa their inclusion in experimental data sets for derivation of such models needs to be critically evaluated .

Supporting Information. Additional information as noted in the text, e.g. illustration of the concept of the isotope method; estimation of the KIE discrimination by diffusion limitation; identificantion of oxidation products; interpretation of product patterns; comparison of inter- and intramolecular KIEs in gas- and water-phase reactions of •OH; collection of KIEs for hydrogen abstraction by •OH in the aqueous and gas phase.

REFERENCES

(1) Mehrjouei, M.; Müller, S.; Möller, D. A review on photocatalytic ozonation used for the treatment of water and wastewater. *Chem. Engineer. J.* **2015**, *263*, 209-219.

(2) Pignatello, J. J. ; Oliveros, E.; MacKay, A. Advanced oxidation processes for organic contaminant destruction based on the Fenton reaction and related chemistry. *Crit. Rev. Environ. Sci. Technol.* **2006**, *36*, 1–84.

(3) Atkinson, R. Kinetics and mechanism of the gas-phase reactions of hydroxyl radicals with organic compounds under atmospheric conditions. *Chem. Rev.* **1986**, *86*, 69-201.

(4) Atkinson, R. Gas-phase tropospheric chemistry of volatile organic compounds: 1. Alkanes and alkenes. *J. Phys. Chem. Ref. Data* **1997**, *26*, 215-290.

(5) Atkinson, R. Atmospheric chemistry of VOCs and NO_x. *Atmos. Environ.* **2000**, *34*, 2063-2101.

(6) Zwiener, C.; Frimmel, F. H. Oxidative treatment of pharmaceuticals in water. *Water Res.* **2000**, *34*, 1881-1885.

(7) Herrmann, H. Kinetics of aqueous phase reactions relevant for atmospheric chemistry. *Chem. Rev.* **2003**, *103*, 4691-4716.

(8) Atkinson, R. Kinetics of the gas-phase reactions of OH radicals with alkanes and cycloalkanes. *Atmos. Chem. Phys.* **2003**, *3*, 2233-2307.

(9) Atkinson, R. A structure-activity relationship for the estimation of rate constants for gas-phase reactions of OH radicals with organic compounds. *Int. J. Chem. Kinet.* **1987**, *19*, 799-828.

(10) Kwok, E. S. C.; Atkinson, R. Estimation of hydroxyl radical reaction rate constants for gas-phase organic compounds using a structure-reactivity relationship: an update. *Atmos. Environ.* **1995**, *29*, 1685-1695.

(11) Buxton, G. V.; Greenstock, C. L.; Helman, W. P.; Ross, A. B. Rate constants for reactions of radicals in aqueous solution. *J. Phys. Chem. Ref. Data* **1988**, *17*, 513-886.

(12) Fokin, A. A.; Schreiner, P. R. Selective alkane transformations via radicals and radical cations: Insights into the activation step from experiment and theory. *Chem. Rev.* **2002**, *102*, 1551-1593.

(13) Monod, A.; Poulain, L.; Grubert, S.; Voisin, D.; Wortham, H. Kinetics of OH-initiated oxidation of oxygenated organic compounds in the aqueous phase: new rate constants, structure-activity relationships and atmospheric implications. *Atmos. Environ.* **2005**, *39*, 7667-7688.

(14) Monod, A.; Doussin, J. F. Structure–activity relationship for the estimation of OH-oxidation rate constants of aliphatic organic compounds in the aqueous phase: alkanes, alcohols, organic acids and bases. *Atmos. Environ.* **2008**, *42*, 7611-7622.

(15) Minakata, D.; Li, K.; Westerhoff, P.; Crittenden, J. C. Development of a group contribution method to predict aqueous phase hydroxyl radical (OH•) reaction rate constants. *Environ. Sci. Technol.* **2009**, *43*, 6220-6227.

(16) Minakata, D.; Crittenden, J. C. Linear free energy relationships between aqueous phase hydroxyl radical reaction rate constants and free energy of activation. *Environ. Sci. Technol.* **2011**, *45*, 3479-3486.

(17) Minakata, D.; Mezyk, S. P.; Jones, J. W.; Daws, B. R.; Crittenden, J. C. Development of linear free energy relationships for aqueous phase radical-involved chemical reactions. *Environ. Sci. Technol.* **2014**, *48*, 13925-13932.

(18) Rudakov, E. S.; Lobachev, V. L.; Volkova, L. K. Cage effects and inverse temperature dependence of the KIE in the c-C_6H_{12}/c-C_6D_{12} reaction with OH radicals in Fenton and HOONO-H_2O Systems. *Int. J. Chem. Kinet.* **2011**, *43*, 557-562.

(19) Elsner, M.; Zwank, L.; Hunkeler, D.; Schwarzenbach, R. P. A new concept linking observable stable isotope fractionation to transformation pathways of organic pollutants. *Environ. Sci. Technol.* **2005**, *39*, 6896-6916.

(20) Frank, J.; Rabinowich, E. Some remarks about free radicals and the photochemistry of solutions. *Trans. Faraday Soc.* **1934**, *30*, 120-131.

(21) Brezonik, P. L. *Chemical Kinetics and Process Dynamics in Aquatic Systems*; CRC Press: Boca-Raton, FL, **1994**, p. 119 ff.

(22) Zegota, H.; Schuchmann, M. N.; von Sonntag, C. Cyclopentylperoxyl and Cyclohexylperoxyl radicals in aqueous solution – a study by product analysis and pulse radiolysis. *J. Phys. Chem.* **1984**, *88*, 5589-5593.

(23) von Sonntag, C.; Schuchmann, H.-P. The elucidation of peroxyl radical reactions in aqueous solution with the help of radiation-chemical methods. *Angew. Chem. Int. Ed.* **1991**, *30*, 1229-1253.

(24) Luo, Y.-R. *Comprehensive Handbook of Chemical Bond Energies*; CRC Press: Boca Raton, FL, 2007.

(25) Pignatello, J. J.; Liu, D.; Huston, P. Evidence for an additional oxidant in the photoassisted Fenton reaction. *Environ. Sci. Technol.* **1999**, *33*, 1832-1839.

(26) NIST Chemical Kinetics Database, Standard Reference Database 17, Version 7.0 (Web Version), Release 1.6.8, Data Version **2013**.03. *A compilation of kinetics data on gas-phase reactions* (http://kinetics.nist.gov/kinetics/index.jsp).

(27) Zhang, N.; Geronimo, I.; Paneth, P.; Schindelka, J.; Schaefer, T.; Herrmann, H.; Vogt, C.; Richnow, H. H. Analyzing sites of OH attack (ring vs. side chain) in oxidation of substituted benzenes via dual stable isotope analysis ($\delta^{13}C$ and $\delta^{2}H$). *Sci. Total Environ.* **2016**, *542*, 484-494.

(28) Bonifacic, M.; Armstrong, D. A.; Stefanic, I.; Asmus, K.-D. KIE for hydrogen abstraction by OH radicals from normal and carbon-deuterated alcohol and methylamine in aqueous solution. *J. Phys. Chem. B* **2003**, *107*, 7268-7276.

(29) Stefanic, I.; Ljubic, I.; Bonifacic, M.; Sabljic, A; Asmus, K.-D.; Armstrong, D. A.; A surprisingly complex aqueous chemistry of the simplest amino acid. A pulse radiolysis and theoretical study on H/D kinetic isotope effects in the reaction of glycine anions with hydroxyl radicals. *Phys. Chem. Chem. Phys.* **2009**, *11*, 2256-2267.

(30) NIST Chemical Kinetics Database, Standard Reference Database 40, *A compilation of kinetics data on solution-phase reactions*, **2002** (http://kinetics.nist.gov/solution/).

(31) Georgi, A.; Polo, M. V.; Crincoli, K.; Mackenzie, K.; Kopinke, F.-D. Accelerated catalytic Fenton reaction with only traces of iron – An Fe-Pd-multicatalysis approach. *Environ. Sci. Technol.* **2016**, *50*, 5882-5891.

(32) Wallington, T. J.; Dagaut, P.; Kurylo, M. J. Correlation between gas-phase and solution-phase reactivities of hydroxyl radicals toward saturated organic compounds. *J. Phys. Chem.* **1988**, *92*, 5024-5028.

(33) Rusevova, K.; Koeferstein, R.; Rosell, M.; Richnow, H. H.; Kopinke, F.-D. $LaFeO_3$ and $BiFeO_3$ perovskites as nanocatalysts for contaminant degradation in heterogeneous Fenton-like reactions. *Chem. Engineer. J.* **2014**, *239*, 322-331.

(34) Zhang, N.; Schindelka, J.; Herrmann, H.; George, C.; Rosell, M.; Herrero-Martin, S.; Klan, P.; Richnow, H. H. Investigation of humic substance photosensitized reactions via carbon and hydrogen isotope fractionation. *Environ. Sci. Technol.* **2015**, *49*, 233-242.

(35) Droege, T. A.; Tully, F. P. Hydrogen atom abstraction from alkanes by OH. 6. Cyclopentane and cyclohexane. *J. Phys. Chem.* **1987**, *91*, 1222-1225.

(36) Hess, W. P.; Tully, F. P. Hydrogen-atom abstraction from methanol by OH. *J. Phys. Chem.* **1989**, *93*, 1944-1947.

(37) Stein, S. E. Comparison of equilibrium constants in gas and liquid phase. *J. Amer. Chem. Soc.* **1981**, *103*, 5685-5690.

TOC Graphic